ISBN: 978-3-95450-220-2 ISSN: 2673-5474 doi: 10.18429/JACoW-FEL2022-WEP25

VIRTUAL DIAGNOSTIC FOR LONGITUDINAL PHASE SPACE IMAGING FOR THE MAX IV SXL PROJECT

J. S. Lundquist*, S. Werin, F. Curbis, Department of Physics, Lund University, Lund, Sweden

Abstract

Accurate and high resolution detection of the Longitudinal Phase Space (LPS) of the electron beam is a great advantage for operating and setting up a FEL. In the case of the soft X-ray FEL being proposed at the MAX IV synchrotron facility in Lund, this information will mainly be supplied by a Transverse Deflecting Cavity (TDC) which is currently being installed and scheduled for commissioning in the autumn (2022). Performing the LPS measurement with the future TDC is limited in two regards: it is destructive and may be low in resolution as compared to the maximum compression possible in the MAX IV linac. In this project we propose using machine learning tools to implement a virtual diagnostic to retrieve the LPS information non-destructively using fast, non-invasive measurements and critical set-points in the linac as inputs for a neural network. In this paper we summarize the current progress of this project which thus far has focused on simulation studies of the TDC and the training of a virtual diagnostic using the TDC's simulated output.

INTRODUCTION

The Soft X-ray Laser (SXL) is a free electron laser currently being proposed as an expansion to the existing synchrotron light facility MAX IV in Lund, Sweden. The SXL is designed as a extension to the operating linac, currently used to drive two electron storage rings as well as a Short Pulse Facility (SPF). The SPF currently hosts only one end-station (FemtoMAX), but two more beamlines are currently planned as new branches at the end of the linac. One is the SXL, where the beam will pass through a 156 m long undulator hall before reaching two experimental end-stations; the other line is reserved for a Transverse Deflecting Cavity (TDC). This is a diagnostic beamline, meant to produce new information of the state of beam, useful for operating the SXL. Figure 1 shows a detailed layout of the MAX IV linac with these proposed beamlines present. The TDC line operates by allowing the beam to pass through a particular accelerating structure which kicks the beam transversely, in order to turn it, in this case horizontally. This allows for a longitudinal image of the beam as it impacts on a screen further down the beamline. One can also pass the beam through a dipole magnetic field before the screen to retrieve information of the energy distribution of the beam. With these two techniques used in tandem one can get a full image of the Longitudinal Phase Space (LPS) of the beam, crucial information for operating the SXL optimally [1].

As the TDC requires the beam to impact on a screen this measurement is destructive and can not be performed in parallel with studies at the SXL beamlines. A non-destructive tool for extracting the same diagnostic information is thus highly attractive. For this project, the possibility of using Machine Learning (ML) methods to develop a virtual diagnostic monitoring this information is being investigated. The virtual diagnostic in this case would interpret non-destructive signals from the entire linac and then produce predictions of the TDC image without interacting with the beam. If this can be achieved with high reliability and accuracy, the operations of the current linac and the future SXL could be significantly improved. Similar projects have shown promising results [2, 3].

In this paper, the early strides of this project are summarized. This includes two main results: predictions of the TDC output based on simulation data and predictions of the beam's transverse image in a dispersive section of the linac based on real data collected during study time on the accelerator. These are referred to as the *simulated* and *experimental* case respectively. The following two sections will go into more detail on the simulation and experiment performed to generate the data used in training the constructed virtual diagnostics, followed by a section covering the machine learning methods used in the virtual diagnostic itself.

DATA COLLECTION

A crucial early step is finding the input channels one could possibly use for training the ML structures. For this project, we require non-destructive, fast measurements which are also correlated to the result of the destructive measurement of the TDC, i.e., they should have a strong dependence or influence on the energy and temporal distribution of the final beam. Below in Table 1 a summary of the different input channels selected, both for the simulation and experimental case, can be seen. Here, L01 refers to a specific early accelerating structure separated from the remainder of the linac by a bunch compressor, L02-19 are then referring to the rest of the 18 accelerating structures which have synchronized setpoints for phase and voltage.

These setpoints were then used as input to different ML structures, either outputting images, or scalar values for the position of the beam centroid. The following two subsections summarize the methods for procuring the data through simulation and experiment.

Simulation

The accelerator simulation code elegant was used for the simulations of the TDC output. Scans were performed of the RF parameters summarized in Table 1, at first systematically to find the limits in each channel, then using 1000 random setpoints from the tested range to produce the final dataset.

* johan.lundquist@maxiv.lu.se

ISBN: 978-3-95450-220-2 ISSN: 2673-5474 doi: 10.18429/JACoW-FEL2022-WEP25

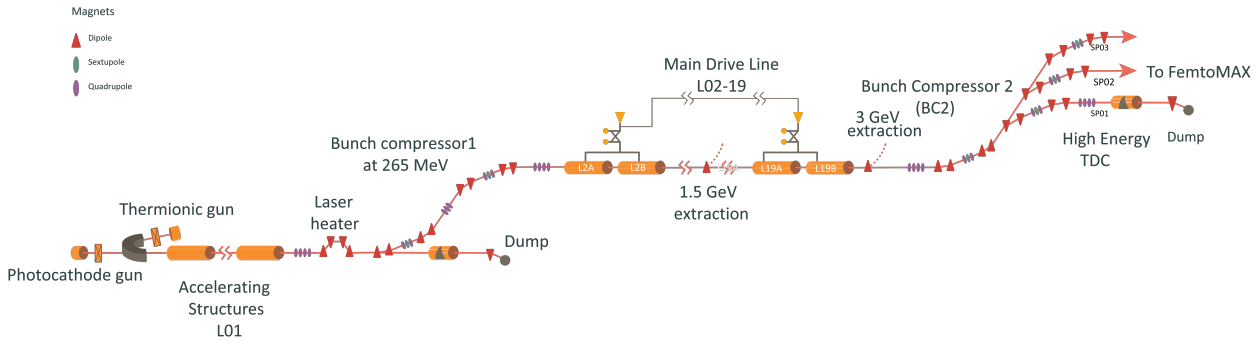

Figure 1: Detailed layout of the MAX IV linac with the currently proposed components of two TDCs and a laser heater, as well as the proposed beamline SP03, going to the SXL.

Table 1: Input Channels from Simulation and Experiment

Simulation	
Input	**Range**
L01 Phase	±20°
L02-19 Phase	±20°
L01 Voltage	±2.5 MV
L02-19 Voltage	±2.5 MV
21 BPMs, X and Y	
Experiment	
Input	**Range**
L01 Phase	170.5-181.5°
L02-19 Phase	2.0-16.0°
L02-19 RF Filltime	2.75-3.15 μs
21 BPMs, X and Y	

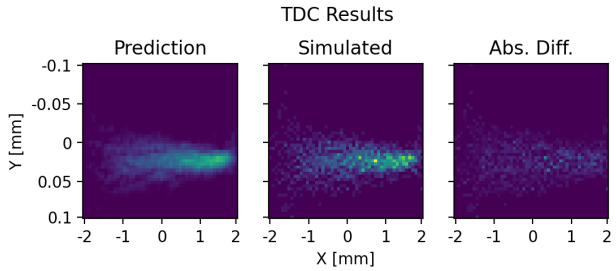

Figure 2: Example of prediction on simulation data for the TDC screen. Leftmost image shows the prediction of the virtual diagnostic, center image shows the corresponding result from the simulation, and the rightmost image shows the absolute difference between the other two.

For each setpoint, 2000 particles were simulated passing through the linac and into the TDC line. Here, the TDC structure itself was on, but the dipole extracting the energy information was deactivated in order to construct a simpler case for the networks to handle. Each setpoint resulted in a change to the temporal distribution of the beam, and thus changing the shape of the beam on the image.

Elegant outputs the transverse position for each of the 2000 particles. This information was reformatted into a 2D histogram of 50 × 50 bins, as to imitate the output of a CCD camera, as will be used in the real TDC beamline. The simulations were set to keep the beam within a 4×0.2 mm^2 area, adjusting the strength of dipole magnets as to retain the central position of the entire beam. An example of the results of this simulation can be seen in the central image of Fig. 2.

Experiment

Beamtime with the MAX IV linac was scheduled to allow the collection of images recorded on a YAG screen in a dispersive section of the second bunch compressor. Such images show the temporal profile of the beam, similar to the process in the TDC beamline. Initial scans of the L01 and main linac phases were performed in steps of 0.5°, then the SLED cavity fill-time of the main linac was stepped through the range indicated in Table 1 in steps of 0.1 μs, with a main linac phase scan performed at each step. For each scan step, 5-10 images were recorded from the YAG screen. In total 1150 images were collected for use in the virtual diagnostic.

The full images were 1200 × 1080 pixels in size, far larger than the simulated 2D histograms. In order to limit the required information contained in the predictions by the networks, these images were sliced down to 200 × 50 pixels. Slicing was done about the point of maximum intensity after the application of a background subtraction and median filtering. In most cases this resulted in a clear image of the entire beam profile, such as the center image in Fig. 4.

VIRTUAL DIAGNOSTIC

The term *virtual diagnostic* in this case refers to an artificial neural network (ANN) mapping the different non-destructive signals from the main linac to the desired images from the TDC, or the screen in the dispersive section of the bunch compressor in the experimental case. An ANN consists of many layered nodes with weighted connections between them. By updating the weights associated with these connections using a defined loss and optimization function, a network can extract the complex mapping between inputs and outputs [5]. For this project, this type of structure will be used to map the connection between specific BPM sig-

ISBN: 978-3-95450-220-2 ISSN: 2673-5474 doi: 10.18429/JACoW-FEL2022-WEP25

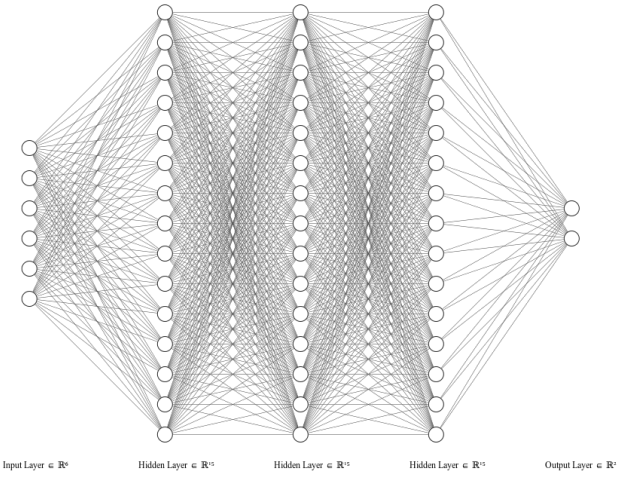

Figure 3: Simplified example of the ANN structure, the circles representing nodes and the lines showing the trainable connections between them. The two output nodes would in this case be the X and Y beam centroid positions. Image constructed using NN-SVG tool [4].

nals and linac setpoints to the outcome of a simulated TDC measurement or to the output of a measured YAG screen image in a bunch compressor.

Two types of networks were constructed for the results in this paper: one type consisting solely of these densely connected nodes for use in predicting the location of the beam centroid on the screen, a simplified example of which can be seen in Fig. 3. The second type of network was constructed with the first few layers being of this same type, densely connected nodes, but with the final layers utilizing a convolutional neural network (CNN) structure. A CNN type of network applies weights to inputs as a matrix of weights moving as a filter across a larger input matrix. The input vector was reshaped into many smaller matrices, which were then put through the convolutional layers. The output matrix from these CNN layers was the final image prediction.

For the simulated results, only the type of network using CNN layers was necessary, as the beam was always centered within the same 4×0.2 mm^2 area, and thus no prediction of the beam centroid was necessary. Here, we utilized a network structure and training parameters as summarized in Table 2.

For the experimental results, the beam was not centered on the intercepting screen, but rather moved across the screen while changing the energy. When the 1200×1080 pixel images were sliced down to 200×50 pixels, the information of where on the screen the beam landed was lost. This is where the simpler ANN structure was utilized, to predict the location of the beam centroid on the screen, while the convolutional type network was used for the image predictions, just as in the simulated case, with a structure and training parameters similar to those summarized in Table 2.

Table 2: Network Structure and Training Parameters

Structure	200 Dense Nodes 200 Dense Nodes 2500 Dense Nodes $100 \cdot 2 \times 2$ CNN Kernels $4 \cdot 4 \times 4$ CNN Kernels $1 \cdot 5 \times 5$ CNN Kernels
Data Sets	1000 Total Images 900 For Training 100 For Predictions
Activation Function	ReLU
Loss Function	Mean Absolute Error
Optimization Algorithm	ADAM
Learning Rate	10^{-3}
Training Epochs	1200
Batch Size	50

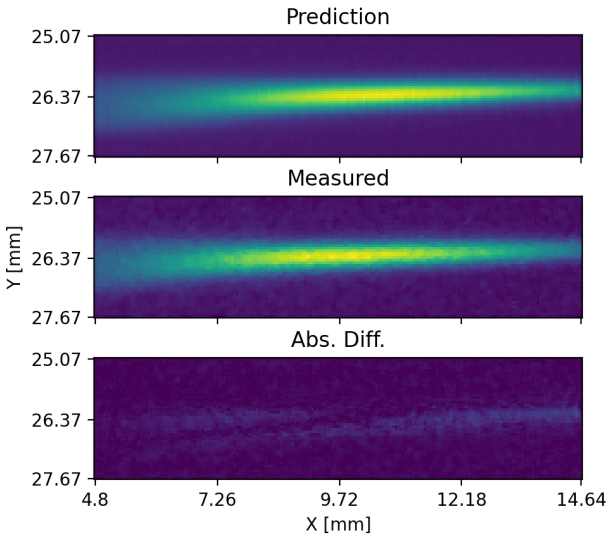

Figure 4: Example of prediction on measured data for the bunch compressor screen. Top image shows the prediction of the virtual diagnostic, center image shows the corresponding measured result, and the bottom image shows the absolute difference between the other two.

RESULTS

Figure 2 shows an example of the results of the *elegant* simulations and the virtual diagnostics' predictions of the TDC output. The leftmost image shows a prediction from the ML model, the center image shows the corresponding result from the simulation, and the rightmost image shows the absolute difference between the other two images. In total, across the 100 images used for predictions, the predictions of the virtual diagnostic reached an RMS error of 12.5 %. The size of the data set could undoubtedly be expanded here, but during simulation the variation in input data was prioritized over volume of images or simulated particles. Furthermore, the particle distributions are simplified by the deactivation of the final dipole magnet extracting the energy distribution.

ISBN: 978-3-95450-220-2 ISSN: 2673-5474 doi: 10.18429/JACoW-FEL2022-WEP25

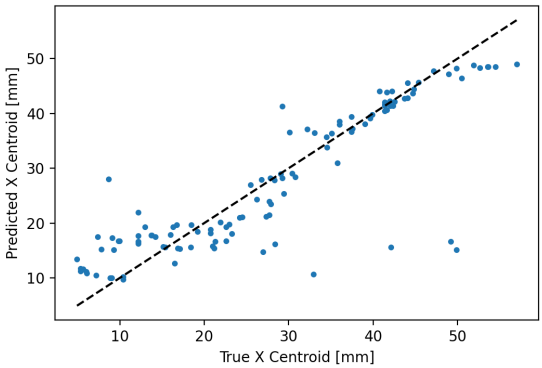

Figure 5: Centroid predictions on real data for bunch compressor screen. The dashed slope one line represents ideal predictions.

For a more complete image of the LPS, the dipole should be activated in future simulations. However, within these limitations we see promising results.

Figure 4 shows an example of the image results of the beamtime and data processing of the experimental results for one set-point, along with an example of the virtual diagnostics' predictions. The top image shows the prediction of the virtual diagnostic for this specific set-point, the center image shows the corresponding measured image on the YAG screen, and the bottom image shows the absolute difference between the other two images. In total, on the 115 measured images saved for predictions, the image predictions of the virtual diagnostic reached an RMS error of 17.3 %. The axes of the prediction image were set using the separate neural network configured to predict the beam centroid on the screen.

Figure 5 shows these centroid predictions, plotted against each prediction's corresponding true value. Thus the ideal virtual diagnostic would form a slope one line, which is also shown in Fig. 5 as the dashed line. Specifically, this figure shows the predictions for the horizontal position of the beam centroid, the axis along which the beam primarily moved with different set-points, as it is the plane of bending for the dipole magnet involved. In total on the 115 centroid positions saved for prediction, the network reached a RMS error of 0.63 mm in the horizontal plane and a RMS error of 1.06 mm in the vertical plane.

OUTLOOK

Virtual diagnostics have been constructed and trained to predict images, both measured and simulated, dependent on the energy and temporal profile of the beam. These predictions have reached a promising level of accuracy with limited time for data collection and training the networks, showing the possibility for the project to develop further in the future. A clear direction is to introduce the energy distribution to the TDC simulations and produce good predictions on such a dataset. Further in the future, the MAX IV TDC should be operational and real measurements can be performed to construct all new datasets for training networks, which could then be used in normal operation of the linac.

REFERENCES

[1] D. Olsson *et al.*, "A Transverse Deflecting Cavity Prototype for the MAX IV LINAC," in *Proc. IBIC'19*, Malmö, Sweden, Sep. 2019, pp. 575–577. doi:10.18429/JACoW-IBIC2019-WEPP025

[2] C. Emma, A. Edelen, M. J. Hogan, B. O'Shea, G. White, and V. Yakimenko, "Machine learning-based longitudinal phase space prediction of particle accelerators," *Phys. Rev. Accel. Beams*, vol. 21, p. 112 802, 2018. doi:10.1103/PhysRevAccelBeams.21.112802

[3] C. Emma, A. Edelen, A. Hanuka, B. O'Shea, and A. Scheinker, "Virtual diagnostic suite for electron beam prediction and control at facet-ii," *Information*, vol. 12, no. 2, 2021. doi:10.3390/info12020061

[4] A. LeNail, "Nn-svg: Publication-ready neural network architecture schematics," *J. Open Source Softw.*, vol. 4, no. 33, p. 747, 2019. doi:10.21105/joss.00747

[5] I. Goodfellow, Y. Bengio, and A. Courville, *Deep Learning*. MIT Press, 2016, http://www.deeplearningbook.org.